

# **Crustal structure from 2-D gravity and magnetic data modeling, magnetic power spectrum inversion, and seismotectonics in the Laguna Salada basin, northern Baja California, Mexico**

Juan García-Abdeslem, Juan Manuel Espinosa-Cardena, Luis Munguía-Orozco, Víctor Manuel Wong-Ortega and Jorge Ramírez-Hernández<sup>1</sup>

*Centro de Investigación Científica y de Educación Superior de Ensenada, División de Ciencias de la Tierra, Ensenada, Baja California, México*

<sup>1</sup>*Universidad Autónoma de Baja California, Instituto de Ingeniería, Mexicali, B. C., México*

Received: August 14, 2000; accepted: April 2, 2001.

## **RESUMEN**

Hemos construido un modelo 2-D de la estructura de la corteza que explica datos aeromagnéticos y de gravedad en un perfil entre la Sierra Juárez y la parte occidental del Valle de Mexicali, cruzando la cuenca Laguna Salada. El modelo ha sido acotado utilizando inferencias independientes acerca de la estructura cortical obtenidas a partir de estudios de refracción sísmica y del modelo Airy-Heiskanen de compensación isostática, mediciones de la densidad de masa y de susceptibilidad magnética en muestras de roca y de un registro de densidad de masa en un pozo, así como con resultados de la inversión del espectro de densidad de potencia de anomalías magnéticas.

Nuestro modelo 2-D sugiere que la Sierra Juárez tiene una raíz que se extiende hasta una profundidad de 42 km y que la interfase corteza-manto alcanza una profundidad de 25 km en la región de la cuenca Laguna Salada, Sierra Cucapá, y la parte más occidental del Valle de Mexicali. La inversión del espectro de potencia y el modelo 2-D sugieren que la base de la corteza magnetizada está a ~16 km de profundidad en la región de la Sierra Cucapá. En el modelo 2-D, la geometría de la cuenca Laguna Salada sugiere una estructura de medio graben, donde el basamento profundiza hacia el oriente, con un relleno sedimentario máximo del orden de 3 km.

La zona sismogénica alcanza una profundidad de casi 20 km, en concordancia con la profundidad inferida a partir del análisis espectral de las anomalías magnéticas. La microsismicidad en la cuenca Laguna Salada ocurre en cúmulos de eventos que indican zonas de debilidad en donde se relajan los esfuerzos. Los hipocentros se localizaron entre 0 y 19.6 km, siendo más profundos en las márgenes de la cuenca, con tendencias que, dentro de los errores de localización, correlacionan bien con el sistema regional de fallas en el área en estudio. Los mecanismos focales determinados evidencian deformación transtensional, en concordancia con el marco tectónico regional.

**PALABRAS CLAVE:** Cuenca Laguna Salada, Baja California, México, gravimetría, magnetometría, modelado 2-D, análisis espectral, seismotectónica.

## **ABSTRACT**

We have constructed a 2-D model of the crustal structure that accounts for gravity and aeromagnetic data across the Laguna Salada basin, using independent inferences from seismic refraction studies and the Airy-Heiskanen model of isostatic compensation, mass density and magnetic susceptibility measurements, a mass density-log from a well, and inversion of the power spectrum from magnetic anomalies. The model suggests that the Sierra Juárez root extends down to about 42 km depth. The crust-mantle interface is at about 25 km depth in the Laguna Salada basin, the Sierra Cucapá, and the western side of the Mexicali valley. The base of magnetized crust is at about 16 km depth under the Sierra Cucapá. The geometry of the basin suggests a half-graben structure dipping eastward. The maximum sedimentary fill is about 3 km thick. The seismogenic zone is about 20 km thick, in good agreement with the depth to the base of the crustal magnetic layer. In the Laguna Salada basin, clusters of events indicate zones of weakness. Hypocenter depths were confined at a depth of up to 19.6 km, being deeper at the margins of Laguna Salada basin. The seismicity pattern correlates well with the regional fault system. Focal mechanisms suggest transtensional deformation in agreement with the regional tectonic framework.

**KEY WORDS:** Laguna Salada basin, Baja California, México, gravity, magnetic, 2-D modeling, spectral analysis, seismotectonics.

## **INTRODUCTION**

The Laguna Salada basin is located in northern Baja California, Mexico (Figure 1). This basin is about 20 km

wide and extends NNW about 100 km to the southwestern end of Imperial Valley, California. The basin is bounded to the west by the Sierra Juárez, which is part of the Peninsular Ranges batholith. The Sierra Juárez has an average altitude

of 1700 m above sea level (m-ASL). To the east, the basin is bounded by the Sierra Cucapá and the Sierra El Mayor, two sub-parallel ranges trending northwest with average altitudes of about 750 m-ASL. Kelm (1971) carried out a gravity survey in the basin and estimated a maximum thickness of sediments of about 6 km in a graben-like structure. The same data set was later re-interpreted by Chavez (1990) with similar results. A tectonic interpretation by Mueller and Rockwell (1991), which largely relied on the Bouguer gravity anomaly of Kelm (1971), proposed a pull-apart model associated with the oblique, right-lateral Laguna Salada fault, where the subsidence in the basin is controlled by an en-echelon arrangement of pull-apart basins.

Over the last decade, the Comisión Federal de Electricidad (CFE) carried out and funded several geological and geophysical studies to evaluate geothermal resources in the Laguna Salada basin. Shallow high temperature was found in the margins of the basin (Espinosa-Cardena, 1986; Arellano-Guadarrama and Venegas-Salgado, 1992). Two gravity surveys, also funded by the CFE, were conducted in a region that includes the Sierra Juárez, the Laguna Salada basin, the Sierra Cucapá, and the western portion of the Mexicali Valley (Ramírez-Hernández *et al.*, 1994; García-Abdeslem and Espinosa-Cardena, 1994). Between 1994 and 1995, CFE drilled three exploratory wells (Figure 1) that found an easterly increase in the thickness of the sedimentary deposits, but no high temperature at depth (Álvarez-Rosales and González-López, 1995).

We have compiled gravity data from several sources, including Velasco-Hernández (1963), Kelm (1971), Ramírez-Hernández *et al.* (1994), García-Abdeslem and Espinosa-Cardena (1994). Aeromagnetic data were obtained from the chart of northwestern México compiled by PEMEX. We construct a 2-D model of crustal structure across the Laguna Salada basin, constrained with: (1) a mass density-log from well ELS-1, located in the western side of Laguna Salada, (2) mass density and magnetic susceptibility measurements of granitic and metamorphic rock samples collected in the Sierra Juárez, the Sierra Cucapá and the Sierra El Mayor; (3) seismic refraction data (Nava and Brune, 1982; Frez *et al.*, 1994), (4) the Airy-Heiskanen model of local isostatic compensation, (5) the thickness of magnetic crust inferred from spectral analysis of magnetic anomalies. The crust-mantle interface was found to reach a depth of about 42 km under Sierra Juárez, and about 25 km toward the east. We suggest that the Laguna Salada basin occupies a half-graben, that reaches a maximum sedimentary fill of about 3 km near its eastern margin.

The results of the seismotectonics study are in good agreement with the regional tectonic framework, providing evidence of transtensional deformation. The seismic activity

suggests that the seismogenic zone extends down to a depth of about 20 km, in agreement with the depth to the base of magnetized crustal layer. These results suggest a normal temperature gradient of about 30° C/km, which is in close agreement with the thermal gradient inferred from temperatures recorded at the bottom of holes drilled by CFE in the Laguna Salada basin

## GEOLOGIC AND TECTONIC SETTING

During the Basin and Range disturbance, in Miocene time, the circum-Gulf region experienced an E-W oriented extensional deformation. This period is characterized by rapid uplifting of the Sierra Juárez and by the development of the Gulf Escarpment along the western margin of the Gulf of California (Angelier *et al.*, 1981; Henry, 1989). Miocene time is also recognized as an intense period of volcanic activity along the margins of the Gulf. The area where simultaneous extension and volcanism took place during the Basin and Range disturbance is primarily the same region where the transform system was later developed (Gastil *et al.*, 1979; Sawlan, 1991; Delgado-Argote and García-Abdeslem, 1999). This last style of deformation has reactivated old Basin and Range structures, overprinting part of the geologic record in the area.

The Laguna Salada basin is located in the NW portion of this extensional province, where many normal faults were reactivated at the beginning of the transcurrent deformation in the western Gulf margin. A generalized geologic map of the study area is shown in Figure 1. The uplifted blocks bordering the Laguna Salada basin includes Paleozoic(?) metasedimentary rocks of amphibolite facies intruded by Cretaceous granitoids of the Peninsular Ranges batholith. The plutonic rocks on both margins, and beneath the sedimentary pile in the basin, range from coarse-grained biotite tonalite to leucocratic granodiorite (Romero-Espejel and Delgado-Argote, 1997; Álvarez-Rosales, 1991; Barnard, 1968; Gastil *et al.*, 1975). In the Sierra El Mayor, the plutonic rocks vary from tonalite to monzogranite and intrude metasedimentary rocks as irregular shaped stocks (Siem, 1992). Miocene volcanic rocks locally overlie the crystalline basement around the basin and its exposed thickness rarely exceed a few tens of meters, however, the Tertiary volcanic deposits are thicker (~ 200 m) in the Sierra Las Tinajas (Figure 1).

Structurally, the escarpment of the Sierra Juárez consists of a discontinuous series of high angle, NNW striking, both east- and west-dipping normal faults across 5 km (Romero-Espejel, 1996; Axen, 1995). The Tertiary volcanic and sedimentary rocks above the granitic basement define an east dipping homoclinal and the range front lacks a major single fault. The major faults lie on the eastern margin of the

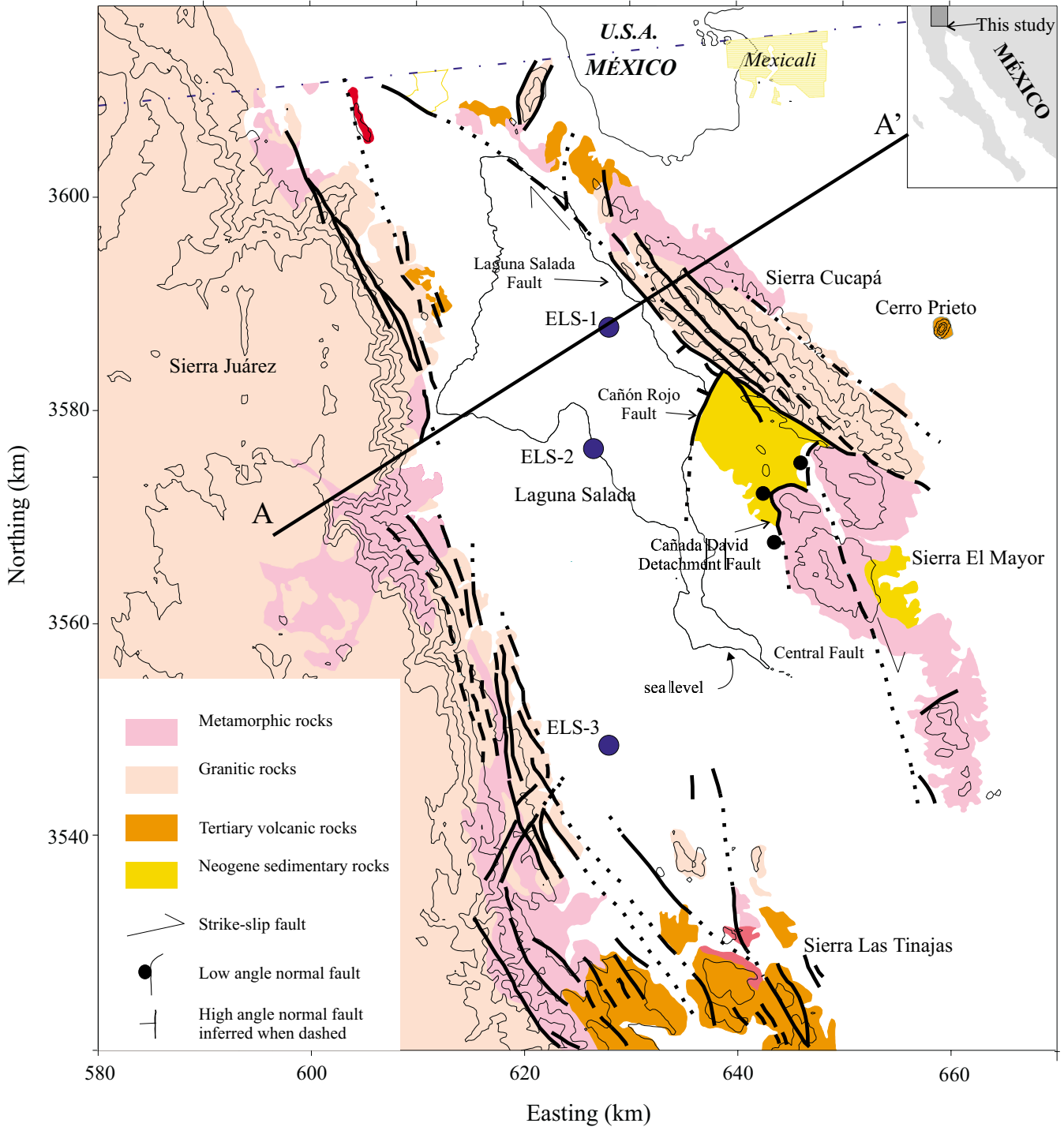


Fig. 1. Geologic map of the study area adapted from INEGI (1980a; 1980b) and Gastil *et al.* (1975). ELS-1, ELS-2, and ELS-3 are exploratory wells drilled by CFE. A-A' indicates the location of the 2-D gravity and magnetic profile.

Laguna Salada basin. The NW-trending, dextral-oblique Laguna Salada Fault is one of the most active faults in the area and it records historic activity (Mueller and Rockwell, 1991). Although this fault is considered part of the San Andreas strike-slip fault system, it has equal amount of normal ver-

sus strike-slip motion for recent times (Muller and Rockwell, 1991). The Cañón Rojo fault merges in the Laguna Salada fault at almost right angle and it is a prominent active normal fault (Figure 1) that acts as a releasing step in Laguna Salada fault system (Mueller and Rockwell, 1991). Based

upon stratigraphic relationships, at least 1200 m of vertical slip has been estimated in the Cañón Rojo fault for Pleistocene time (Vázquez-Hernández, 1996; Dorsey and Martín-Barajas, 1999). The Cañada David detachment fault (Figure 1) indicates that extension was important in late Miocene-Pliocene time. This apparently inactive fault segment juxtaposes late Neogene-Pleistocene(?) sedimentary deposits and metamorphic basement (Siem and Gastil, 1994; Vázquez-Hernández, 1996).

A sequence of terrigenous sediments, about 850 m thick, is exposed in the eastern margin of the Laguna Salada basin, north of the Sierra El Mayor (Vázquez-Hernández, 1996). At the base of this sequence is a ~310 m thick sedimentary unit, constituted by conglomerates, mudstons, and fine grained sandstones, likely correlated with the Imperial Fm., resting in unconformity by a low angle normal fault on igneous and metamorphic rocks. Locally, the Imperial Fm. is representative of an outer shelf-continental slope depositional environment. In the middle of the sedimentary sequence is a ~170 m thick unit, likely correlated with the Palm Spring Fm., constituted mainly of arkosic sandstones deposited in a deltaic environment. At the top of this sedimentary sequence is a ~360 m thick unit that include alluvial fan deposits known as the Cañón Rojo fanglomerate, conglomerate, and breccia. This sedimentary sequence is important because it provides information from the lower sedimentary section in the Laguna Salada basin.

### DRILLHOLES

Three geothermal exploratory wells (Figure 1) drilled in the Laguna Salada basin by the CFE (Álvarez-Rosales and González-López, 1995), indicate a thicker sedimentary fill eastwards. The well ELS-3, located in the southwest side of the Laguna Salada basin, reached metamorphic basement after drilling ~900 m of sedimentary rocks. In the central part of the Laguna Salada basin well ELS-2 traversed a sedimentary section of ~1300 m and cut granitic basement rocks. The well ELS-1, located close to the LSF, is the deepest hole (2404 m) and it traversed three main sedimentary sections (Figure 2). From top to bottom it starts with a first section comprising 980 m of fine-grained lacustrine and fluvial deposits constituted by sand, gravel and shale. The second section, from about 980 to 1830 m depth, includes several sequences of silts and sandstones, interrupted by four layers of about 100-300 m thick granitic boulder-conglomerate and breccia. The third section is constituted by a sequence of about 570 m of fluvial arkosic sediments likely correlated with the Palm Spring Fm. Although the basement was not reached in the well ELS-1, a minimum of ~300 m-thick deposits of the Imperial Fm. is inferred to underlie the Palm Spring Fm. sediments recorded in this well, as exposed east of the basin (Vázquez-Hernández, 1996). Thus, direct ob-

servations indicate a thickness of about 2700 m of early Pliocene to Recent deposits in the eastern margin of the Laguna Salada basin. A detailed study of fossil spores in the stratigraphic sequences of well ELS-1 can be found in Helenes-Escamilla (1999).

The pull-apart model of Mueller and Rockwell (1991) needs a higher than normal geothermal gradient at the central part of the basin, and eventually a western structural boundary. However, the bottom temperature recorded in the exploratory wells drilled by the CFE at the Laguna Salada basin depict an easterly temperature increase, suggesting a normal geothermal gradient in wells ELS-3 (27.2° C at 898 m depth) and ELS-2 (74.3° C at 1755 m depth), and a slighter higher than normal geothermal gradient (124° C at 2404 m depth) in the ELS-1 over the eastern margin of the Laguna Salada basin (Álvarez-Rosales and González-López, 1995).

### SEISMOTECTONICS

The seismotectonics study of the Laguna Salada basin was carried out in two field seasons. During the first season, a five-station network consisting of smoked-paper seismographs and 1-Hz vertical seismometers was deployed in the northern portion of the Laguna Salada basin (stations E1 through E6 in Figure 3). In that area, the network was maintained in operation from July to December 1991. For the second season, the seismic stations were installed further south within the Laguna Salada basin (stations E6 through E10 in Figure 3) for another five-month recording period (April to September 1992). Several hundred micro-earthquakes with magnitudes up to 3.58 were recorded by the networks. However, due to the low magnitude of most of the recorded events, only a limited number of epicenters were properly located. Figure 3 shows the epicenters for about 300 micro-earthquakes that were located with errors of less than 3 km, in both epicenter and focal depth. From this figure, it may be noticed immediately that the overall seismicity does not occur randomly in the area. It rather develops as clusters of events that are inferred to be zones of weakness, along which stresses are being released. The following specific features, related to small and localized clusters of activity, may be observed in Figure 3. Notable zones of micro-earthquake activity are located along the Laguna Salada fault (around station E1), south-southeast of the Cañón de Guadalupe (around station E7), in zones located between stations E2 and E5, and between stations E3, E4, and E6. Besides the significant active faulting that characterizes the first two of the indicated zones, shallow high temperature measurements and hydrothermal activity have also been reported (Espinosa-Cardeña, 1986). An additional zone of high seismic activity was located just west of the Cerro Prieto geothermal field (close to station E10). This zone, however, is outside the area of main interest for the present study.

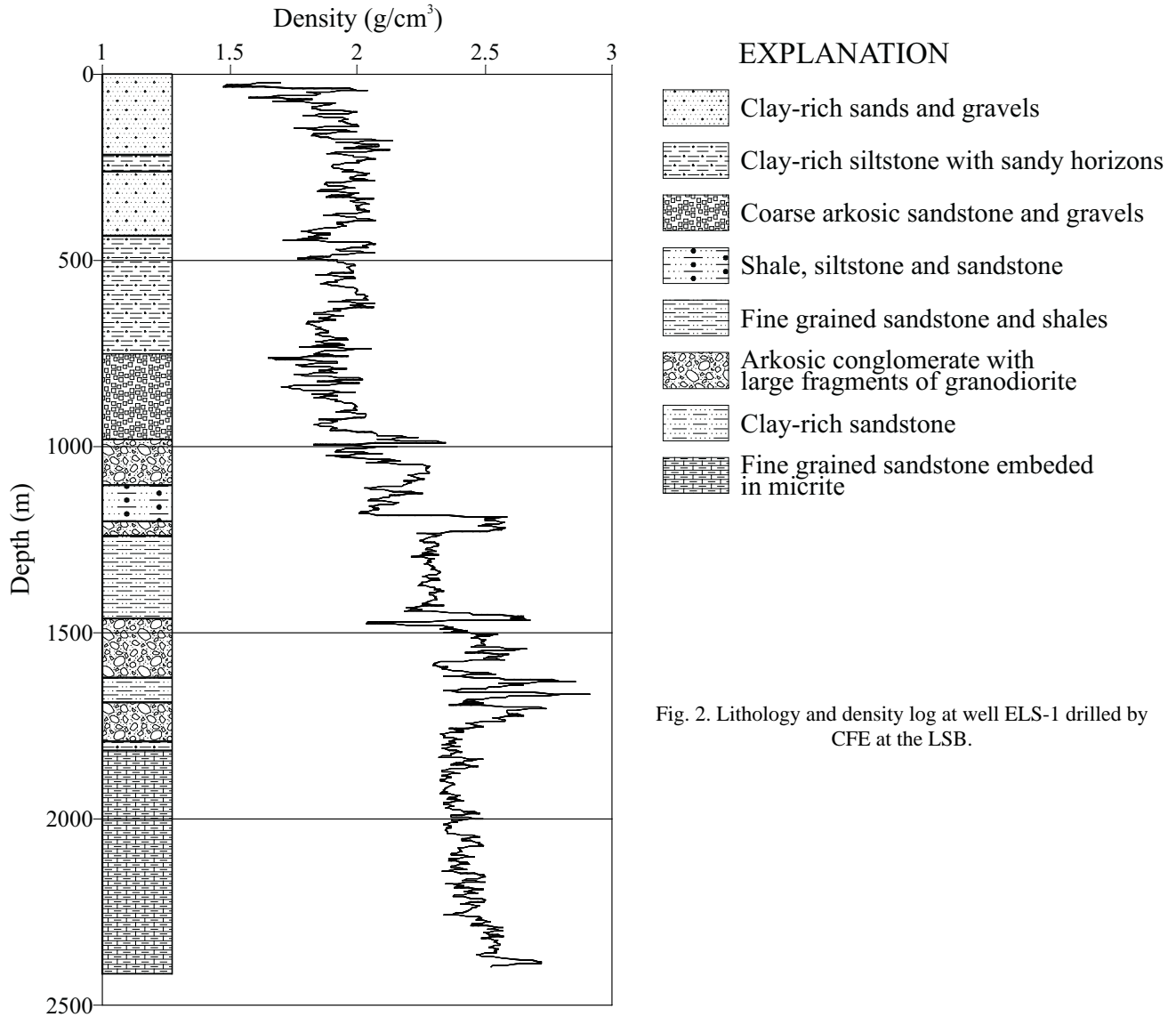


Fig. 2. Lithology and density log at well ELS-1 drilled by CFE at the LSB.

Regarding hypocenter depths, micro-earthquakes occurring in the central part of the Laguna Salada basin (close to stations E2, E3, E4, E5, and E6) were mostly confined within a depth range of 0 to 6 km. The epicenters observed in the vicinity of the stations E6, E7 and E8 had sources at depths from 2 to 12 km, while focal depths for events clustered around the station E1 ranged from 6 to 19.6 km. Events deeper than 12 km were located mainly in the regions of Sierra Cucapá, the western part of The Mexicali Valley, the western front range of Sierra Juárez, and 17 events at the Laguna Salada basin.

Estimates of  $b$ , the slope in the frequency-magnitude linear relationship  $\text{Log } N = a - b M$  (Scholz, 1968), for the zones of high seismic activity are between 1.12 and 1.60, suggesting highly fractured zones with low levels of local stress. The fact that the recorded events are spatially clus-

tered is an indication of anomalous zones in which tectonic stress accumulates and releases repeatedly.

Composite fault plane solutions were also determined for selected groups of events. These solutions were prepared with P-wave first motion data, from events having duration magnitudes between 2.1 and 3.58, with epicenters spatially separated by no more than 3 km, and focal depths shallower than 8 km. Different type of mechanisms were obtained, reflecting in this manner the structural complexity of the zone. Focal mechanism solutions (Figure 3) marked with letters H, and M for events located at the basin margins, are of the oblique-slip normal type of motion, suggesting NNW-SSE and NNE-SSW compressional and dilatational stress axes, respectively. Fault plane solutions indicated with letters A, C, E, F, and L exhibit thrust faulting, while solutions D and K show either right- or left-lateral oblique faulting. Although

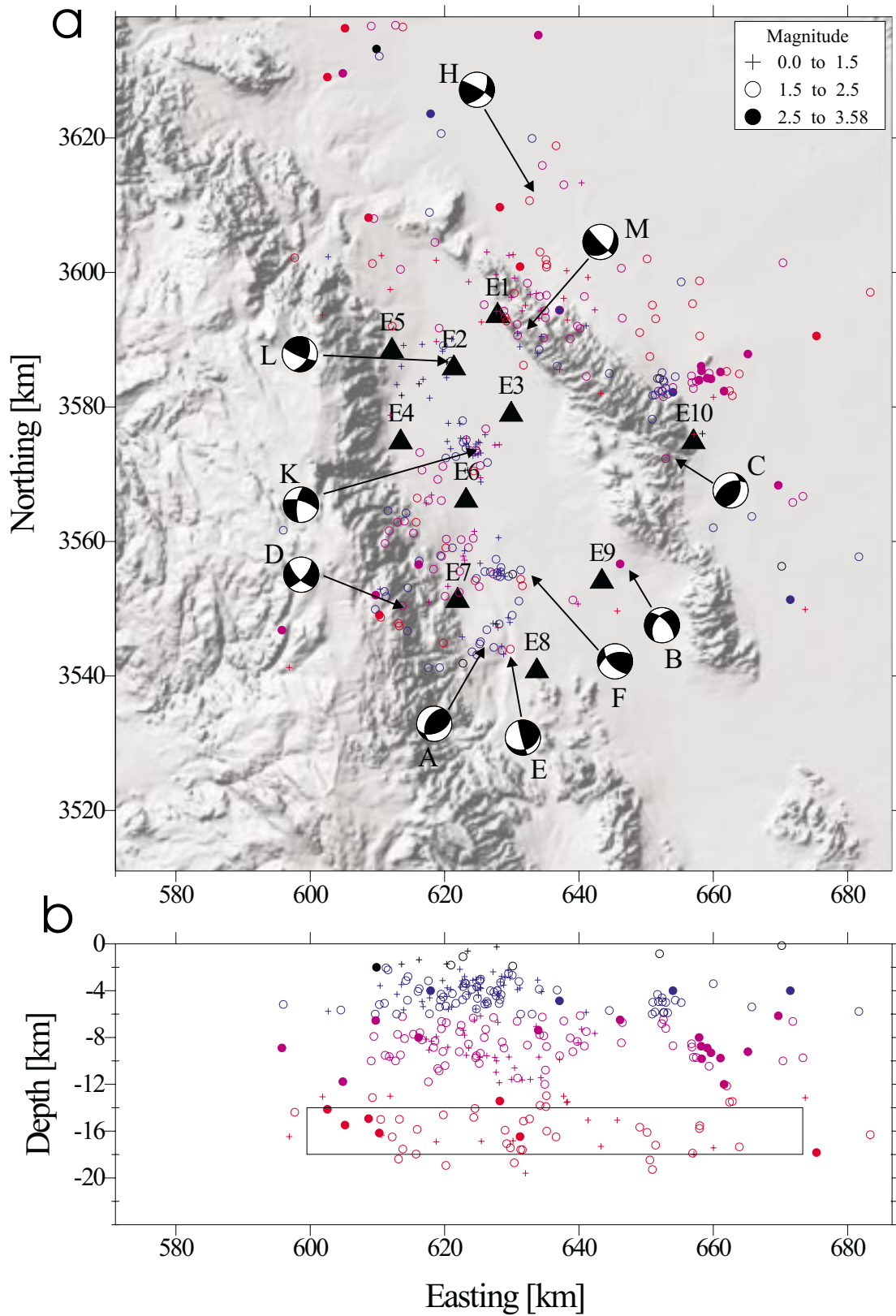


Fig. 3. (a) Seismicity observed in the Laguna Salada Basin and adjacent areas. The solid triangles denote the location of the seismic network. Duration magnitudes were divided into three groups as indicated in the figure. (b) The distribution of seismic events along an W-E profile suggests that the seismogenic zone extends down to a depth of about 20 km. The rectangle at  $16 \pm 2$  km depth denotes the depth to the base of the magnetized crust, inferred from the spectral analysis of magnetic anomalies. The key of colors is as follows: black symbols denote hypocenter depths between 0-2 km, blue between 2-6 km, magenta between 6-12 km, and red between 12-19.6 km.

these fault plane solutions are not as precise as desirable due to the limited number of P-wave polarities used, in general they provide evidence of transtensional deformation, which is in agreement with the regional tectonic regime.

The hypocenter depths for the study area, shown in Figure 3 along an E-W profile, suggest that the seismogenic zone comprises an about 20 km thick layer. Within the seismogenic zone the crust behaves as a brittle material, that fails when subjected to stresses greater than the strength of the material, which depends on both temperature and pressure. For temperatures above 600°C those materials that could realistically make up the continental crust will begin to experience ductile deformation (Lay and Wallace, 1995). This suggest a normal gradient of temperature with depth of about 30°C/km, in close agreement with the temperatures recorded at the bottom of exploratory holes drilled by CFE in the Laguna Salada basin

## GRAVITY AND MAGNETIC DATA DESCRIPTION

All of the gravity data used in this study were tied to absolute gravity at the gravimetric base located at the Rodolfo Sánchez Taboada monument in Mexicali, and referred to the IGRS-67. Using a Bouguer mass density of 2670 kg/m<sup>3</sup>, a complete Bouguer anomaly was obtained for the Laguna Salada basin and adjacent areas (Figure 4). Total field aeromagnetic data were digitized from the Aeromagnetic Chart of Northwest México, from a survey flew by PEMEX at about 1800 m-ASL. These data were detrended to obtain the residual total field magnetic anomaly shown in Figure 5. In the following paragraphs, we discuss its possible significance and its relationship with the main geologic features.

### The complete Bouguer gravity anomaly

The Bouguer gravity anomaly at the Sierra Juárez varies, from north to south, between -50 and -75 mGals, showing a strong negative correlation with topography, indicating the presence of a root under the Sierra Juárez. In this region, the gravity anomaly suggests either a slight southward decrease in the density, or a local deepening of the root.

At the Laguna Salada basin, the Bouguer gravity anomaly shows a prominent minimum extending in NNW direction along some 50-60 km. It is evident that its origin is due to the large density contrast between the sedimentary blanket that fills the basin and the surrounding crystalline basement. At the center of the basin, this minimum reaches about -65 mGals. The western and eastern sides of the basin have contrasting gravity styles. The transition region from the eastern margin of the Sierra Juárez towards the Laguna

Salada basin features a smooth, horizontal gravity gradient, suggesting a similar density in the rocks of the basement, and the absence of major structural disruptions. A remarkable difference is observed at the eastern margin of the Laguna Salada basin, where an intense horizontal gravity gradient extends along some 60-km over the western margins of the Sierra Cucapá and the Sierra El Mayor. This is one of the most prominent features in the Bouguer gravity anomaly, which is interpreted as a major structural disruption caused by an abrupt lateral change in density through the Laguna Salada fault and the Cañada David detachment fault.

The Bouguer gravity anomaly shows maximum values (0 mGals) in Sierra El Mayor. This feature extends towards the N-NW along some 20 km and may be associated with a metamorphic core complex (Siem, 1992). In the Mexicali Valley, the Bouguer gravity anomaly features several short wavelength anomalies suggesting abrupt but local changes in the thickness of sediments. It is inferred that the horizontal gradient observed is caused by lateral changes in density nearby the Imperial fault, to the northeast of the Cerro Prieto volcano.

### Residual total field aeromagnetic anomalies

Several features of the residual total field aeromagnetic anomaly (Figure 5) are worth describing. Over the southern end of the Laguna Salada basin, the field remains almost featureless. Notice however a relative magnetic high occurring in the northern part of the basin, suggesting a region where the basement is shallower. The magnetic anomaly shows increasing values towards the northeast, where a strong anomaly reaching up to 120 nT is located just over the Sierra Cucapá. Another 80 nT magnetic high, coinciding with a -10 mGals gravity high, is located east of the Sierra Cucapá, towards the northeast of the Cerro Prieto volcano. This anomaly is bounded by a steep gradient, which is also coincident with the gravity gradient located just over the trace of the Imperial fault. The dipole anomaly partially shown over the eastern side of the study area, is observed also on ground magnetic data; it is known as the Nuevo León magnetic anomaly after Fonseca and Razo-Montiel (1979). This magnetic anomaly has been interpreted by several authors as due to a gabbroic source body: Goldstein *et al.* (1984) suggest that the top of the source body lies at 3.8 km depth. The interpretation by Quintanilla and Suárez-Vidal (1994) suggest a depth to the top of the source body at about 4.5 km.

Additional ground magnetic data can be found in Kelm (1971), who measured the vertical component of the earth's magnetic field in the Laguna Salada basin. However this study had several problems during its execution that rule out its use. Kelm (1971) used an Askania magnetometer with

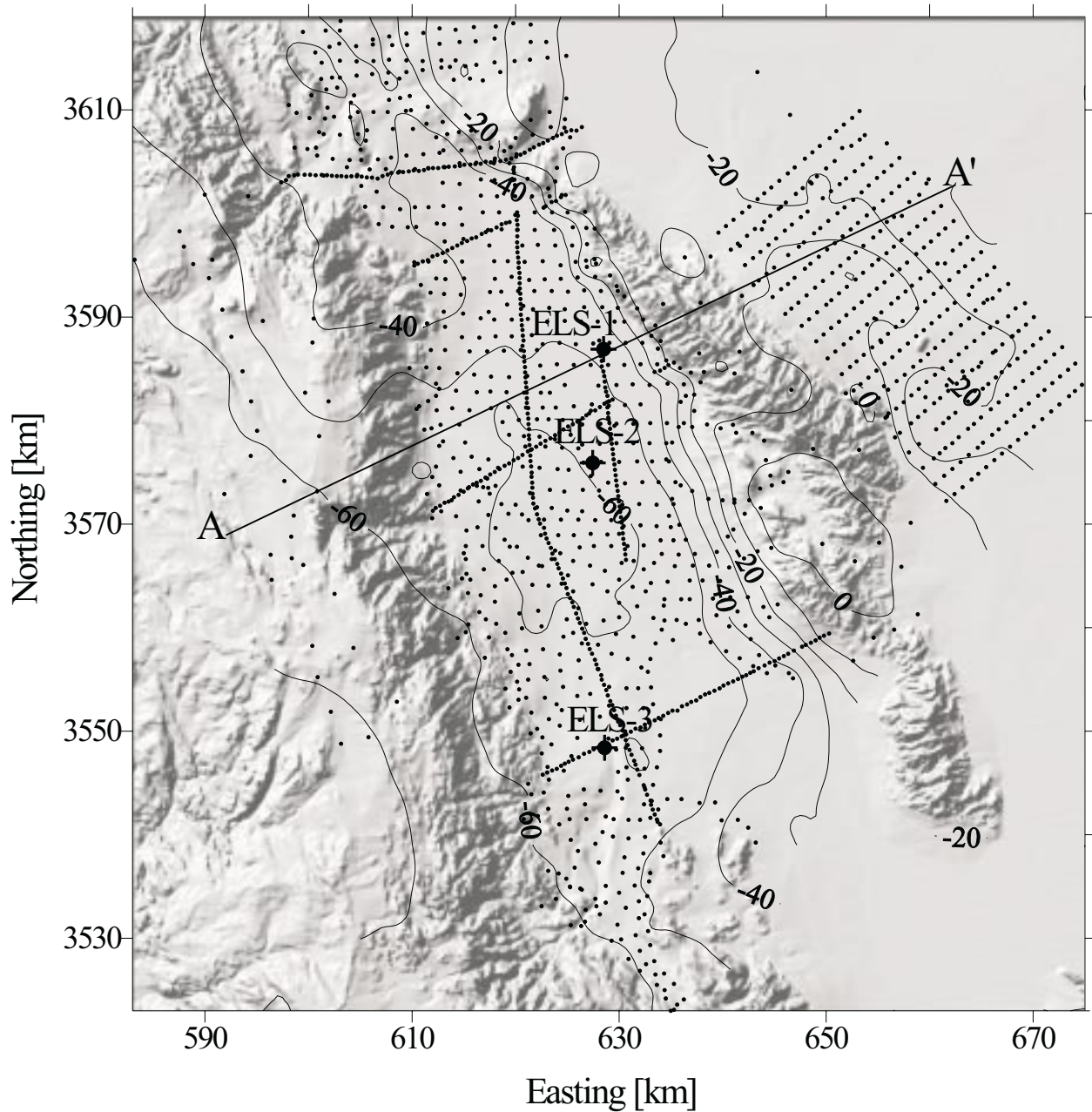


Fig. 4. Shaded relief map of the study area showing the complete Bouguer gravity anomaly with contours every 10 mGals, computed using a Bouguer density of  $2670 \text{ kg/m}^3$ . The dots indicates the location of gravity stations. A-A' indicates the location of the 2-D gravity profile.

a reliability of about 5 nT, and instrumental drift equivalent to 100 nT/h at temperatures over  $40^\circ\text{C}$ . Therefore, as mentioned by Kelm (1971): at a base station it was impossible to distinguish whether this change was due to instrumental drift or due to geomagnetic field change.

### SPECTRAL ANALYSIS

With the aim of obtaining a rough estimate of the geometry of the crustal magnetic layer, the inversion of the

radially-averaged (RA) power density spectrum (PDS) of magnetic anomalies was carried out in the region around Sierra Cucupá (Figure 5), following a method described in García-Abdeslem and Ness (1994a, 1994b). For this purpose, the magnetic anomaly was gridded using a minimum curvature algorithm with samples spaced 1 km, tapered at its edges with a 20 point cosine square window, and appended with zeroes to obtain a  $128 \times 128$  regular grid. The natural logarithm of the power spectrum was computed using a 2-D discrete Fourier transform algorithm (Figure 6), it was normalized with respect to the DC component to obtain the PDS,



and then averaged in concentric annulus to obtain the RA-PDS.

In this method we assume that the crustal magnetic field is due to one ensemble of randomly located and uniformly magnetized prisms. The RA-PDS of the crustal magnetic field is modeled using a functional that statistically describe depth, thickness and horizontal dimensions of prisms in the ensemble. The RA-PDS of the study area was inverted using a nonlinear discrete inverse method that is based in the ridge-regression algorithm. It depends on an initial set of values

for the model parameters, that are iteratively modified in order to reduce the misfit between the observed and computed spectrum. Figure 7 shows the RA-PDS data and the model response that yield the inverse method, after 38 iterations, with a *rms* misfit between the observed and computed spectra of about 1.59%, where:

$$rms = 100 \times \sqrt{\frac{\sum (\text{Observed} - \text{Computed})^2}{\sum (\text{Observed})^2}} \quad (1)$$

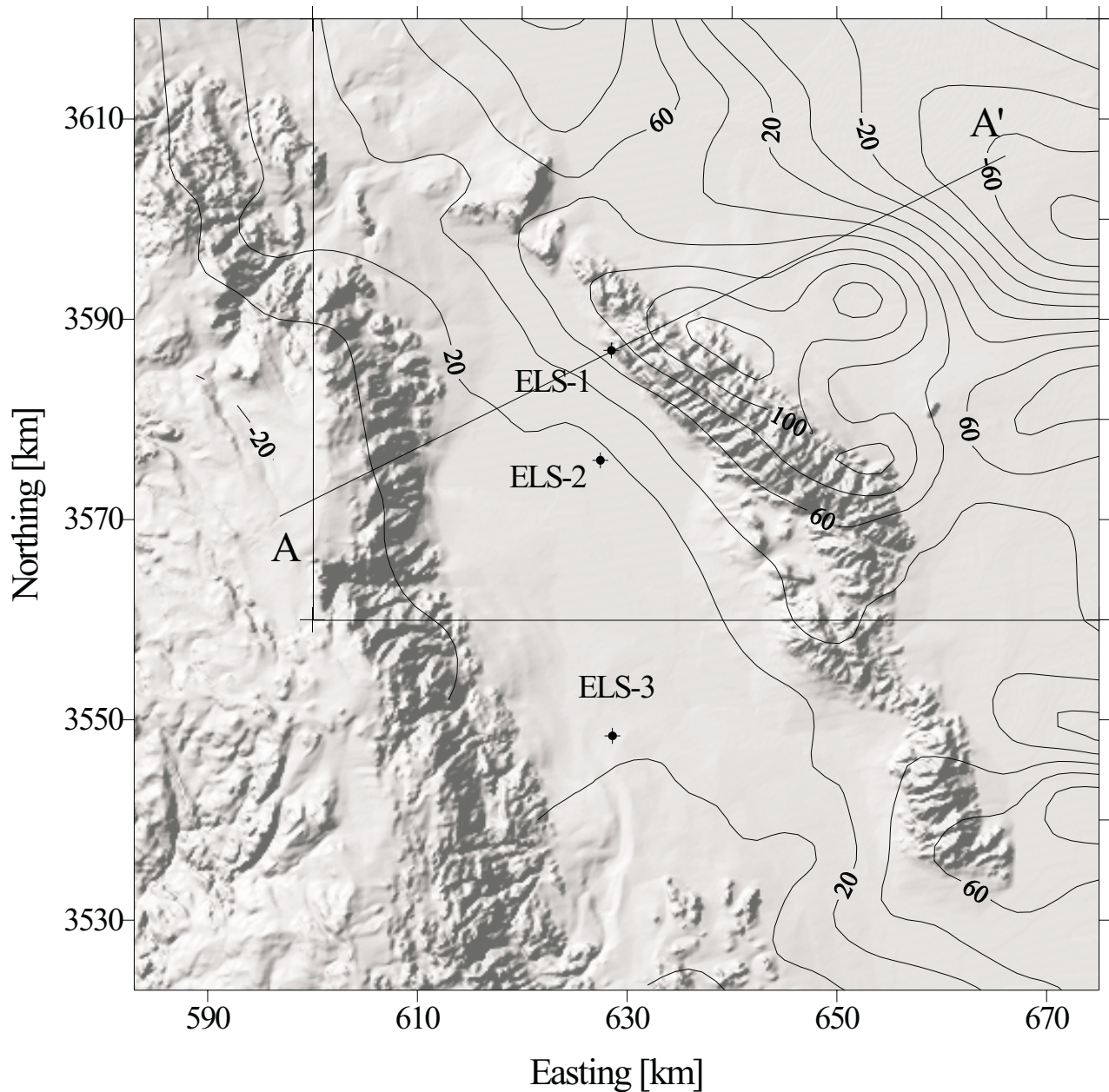


Fig. 5. Shaded relief map of the study area showing the total-field residual magnetic anomaly with contours every 10 nT. The data were collected at an altitude of 1800 m-ASL. The square indicates the region selected for spectral analysis. A-A' indicates the location of the 2-D magnetic profile.

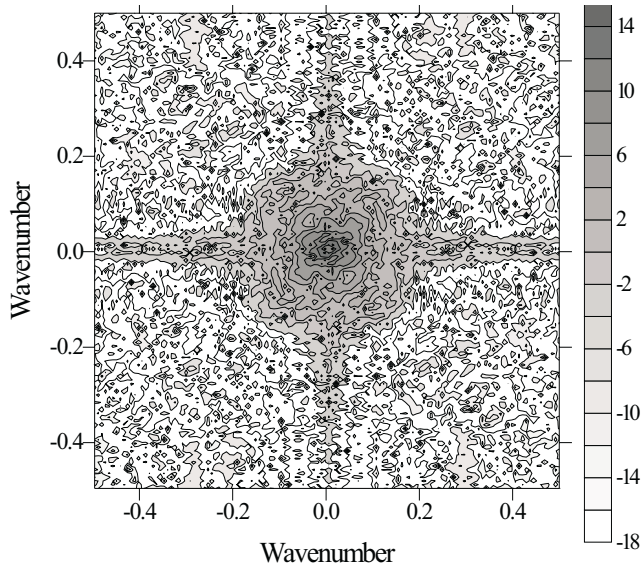


Fig. 6. PDS of magnetic anomalies from the square in Figure 5.

The model parameters obtained are listed in Table 1. The aeromagnetic survey was carried out at an altitude of 1.8 km-ASL. Therefore, the results of this inverse method suggest that the mean depth to the top of the magnetized crust is at about 0.8 km-BSL, and its bottom is at about  $16 \pm 2$  km-BSL, which can be interpreted either as a lithological boundary between magnetic material on top of non-magnetic material, or as the Curie point isotherm depth.

The magnetic susceptibility and strength of the materials that make up the continental crust are factors controlled by temperature. For temperatures higher than the Curie point, magnetic ordering is loose and both induced and remanent magnetization vanish, while for temperatures greater than  $600^\circ\text{C}$  those materials will begin to experience ductile deformation. The inferred depth to the base of the crustal magnetic layer lies at the base of the seismogenic zone shown in Figure 3. This suggests that magnetite, with a Curie point temperature of  $\sim 580^\circ\text{C}$ , carries the magnetization, that the Curie point isotherm depth nearly follows the brittle-ductile transition, and a normal gradient of temperature with depth of about  $30^\circ\text{C}/\text{km}$ .

### CONSTRAINTS

The four layers crustal model inferred by Nava and Brune (1982) from a reverse refraction line across the Peninsular Ranges suggests a crust with the following characteristics. The upper crust consists of two layers: a 5-km thick layer, with P-wave velocity  $\alpha = 5600$  m/s, on top of a 15 km-thick layer with seismic velocity  $\alpha = 6600$  m/s. The lower crust in the model is about 22-km thick, extending from about

20 to 42 km depth and P-wave velocity  $\alpha = 7000$  m/s. Underlying this last unit is the mantle with seismic P-wave velocity  $\alpha = 8000$  m/s. A crustal thickness of about 25 km was interpreted by Frez *et al.* (1994) from a refraction line along the Pacific coast of northern Baja California. A similar value for the crustal thickness at sea level (24 km) was interpreted by O'Connor and Chase (1989) from gravity data across the Baja California Peninsula at the Sierra San Pedro Mártir, that is the highest elevation in the Peninsula, located south of the present study area. These inferences of crustal thickness will be used to constrain the geometry of a 2-D gravity and magnetic model.

A rough estimate of the density contrast at the crust-mantle interface may be obtained by using the Airy-Heiskanen model of local isostatic compensation (Blakely, 1995). In the application of this model to determine the geometry of the crust-mantle boundary we assume that isostatic equilibrium has been reached and that compensation is local. This model requires the selection of values for three parameters: a depth of compensation at sea level ( $d_s$ ), a density contrast through the base of the root ( $\Delta\rho$ ), and a density for the topographic load ( $\rho$ ). These parameters define the depth ( $d$ ) to the base of the root in continental areas by the relationship

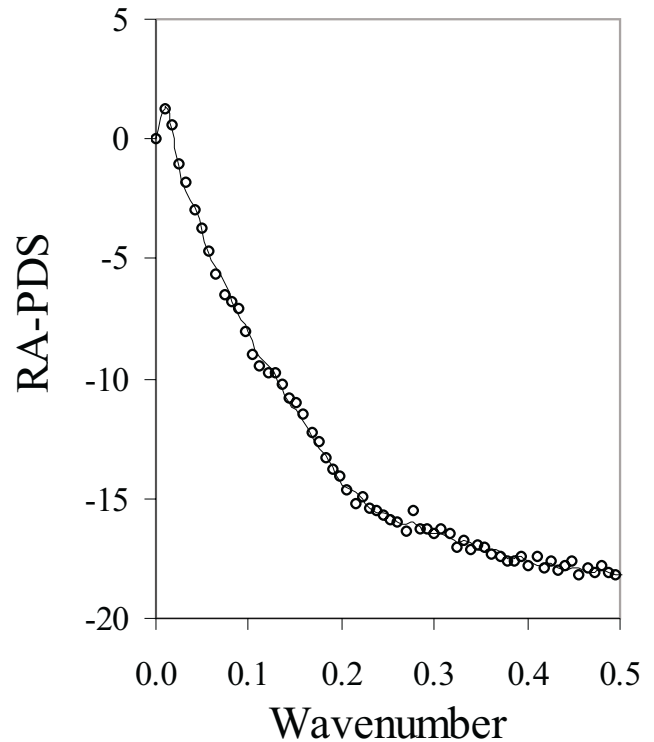


Fig. 7. Indicated with circles is the radially-averaged power density spectrum (RA-PDS) of magnetic anomalies from the region indicated in Figure 5. Continuous line is the model response that results from the inversion of the RA-PDS.

**Table 1**

Results of the RA-PDS inversion. Depth is measured from 1.8 km-ASL

Description of the ensemble parameters	Parameter [km]	Standard deviation [km]
Normally distributed mean depth to top	$h = 2.609 \pm 0.084$	$\sigma_h = 0.977 \pm 0.025$
Mean thickness	$t = 15.110 \pm 2.081$	
Uniformly distributed horizontal EW-length	$a = 34.23 \pm 2.081$	$\Delta_a = 18.30 \pm 0.147$
Uniformly distributed horizontal NS-length	$b = 34.08 \pm 0.439$	$\Delta_b = 18.84 \pm 0.234$

$$d = d_s + e(\rho_t / \Delta\rho), \quad (2)$$

where  $e$  is elevation above sea level. Considering an average elevation  $e = 1700$  m at the Sierra Juárez, and a depth of compensation at sea level  $d_s = 25$  km, in agreement with the thickness reported by Frez *et al.* (1994), to obtain a maximum depth similar to the one reported in Nava and Brune (1982), the density contrast across the crust-mantle boundary has to be close to  $\Delta\rho = -250$  kg/m<sup>3</sup>.

Additional independent information, regarding densities and thickness of sedimentary layers in the Laguna Salada basin, was taken from a density log in well LSE-1 (Figure 2). In addition, mass density and magnetic susceptibility measurements (Appendix A) were carried out in metamorphic and granitic rock samples collected in the Sierra Juárez, the Sierra Cucapá, and the Sierra El Mayor. The statistic analysis carried out in the whole population (130 samples) indicates a normally distributed mass density that ranges between 2400 – 2990 kg/m<sup>3</sup> with an average of about  $2650 \pm 90$  kg/m<sup>3</sup>. The low end members of this population are, in general, weathered granitoids and gneisses. Density measurements from schist outcrops range between 2390 – 3240 kg/m<sup>3</sup>, where the highest values correspond to samples from La Rumorosa, located north of the Sierra Juárez, and from the Sierra El Mayor. The mass density in gneiss and amphibolite outcrops vary between 2550 – 2560 kg/m<sup>3</sup> and 2610 – 3050 kg/m<sup>3</sup>, respectively, where the highest density is from samples collected in the Sierra El Mayor.

Statistic analysis of magnetic susceptibility, carried out in a population of 148 samples, shows a log normal (geometric) distribution that ranges between  $2.00 \times 10^{-5}$  to  $1.6 \times 10^{-3}$  SI units, with a geometric mean magnetic susceptibility of about  $1.75 \pm 2.71 \times 10^{-4}$  SI units. Magnetic susceptibility measurements by de Boerd (1979) in granodiorite samples from Sierra Cucapá vary between  $1.59 \times 10^{-4}$  to  $4.77 \times 10^{-3}$  SI units. The Koenigsberger ratio reported by de Boerd (1979) varies between 0.02 and 0.2. These last results suggest that a

valid assumption is to consider magnetization as due to induction in the local direction of the earth's magnetic field.

## 2-D GRAVITY AND MAGNETIC MODEL

This section describes the interpretation of complete Bouguer gravity and magnetic anomalies based upon a 2-D model along a transect that begins at the Sierra Juárez and ends at the western side of the Mexicali Valley, north of the Cerro Prieto volcano (Figure 1). This interpretation was made using the line-integral method (Hubert, 1948). We use polygons of constant mass density and magnetic susceptibility, assuming that magnetization is due to induction in the local direction of the earth's magnetic field. The model is bounded on top by topography, and it extends *ad infinitum* in the direction perpendicular to the transect strike. The 2-D model, shown in Figures 8 and 9, that extends from the Sierra Juárez to the Mexicali Valley along the profile A-A' indicated in Figure 1, shows the crustal structure in terms of the mass density and magnetic susceptibility that explain the Bouguer gravity and magnetic anomalies.

The following major features of the 2-D gravity and magnetic model are shown in Figure 8. The uppermost crustal layer, which includes the Sierra Juárez and the Sierra Cucapá, was modeled using a mass density of 2670 kg/m<sup>3</sup> and magnetic susceptibility of  $1.75 \times 10^{-4}$  SI units (Appendix A). This layer extends down up to 7 km depth under the Sierra Juárez, constitutes the Laguna Salada basin basement, it thins out eastwards under the Sierra Cucapá, and it is the basement in the Mexicali Valley. Underlying this unit, is a layer located mainly under the Sierra Juárez and the Laguna Salada basin, that was modeled using a mass density of 2740 kg/m<sup>3</sup> and magnetic susceptibility of  $1.75 \times 10^{-4}$  SI units. It has a maximum thickness of about 9 km under the Sierra Juárez and thins eastwards, and its eastern limit is located nearby the Laguna Salada fault in the western front range of the Sierra Cucapá. Underlying this last unit, is a layer that extends down to about 19 km depth, which was modeled us-

ing a mass density of 2700 kg/m<sup>3</sup> and magnetic susceptibility of about  $1.0 \times 10^{-2}$  SI units. It is worth to point out that this last unit has the largest magnetic susceptibility in the 2-D model, being responsible for most of the magnetic anomaly. Considering an empirical law by Balsley and Buddington (1958) this unit is equivalent to a rock with about 0.5 percent in volume of magnetite, and its mean depth to bottom is in good agreement with the one obtained from the RA-PDS inversion. The lower crust was modeled using two layers, with a mass density of 2850 kg/m<sup>3</sup> and 3050 kg/m<sup>3</sup>, respectively, and null magnetic susceptibility. It extends down to a depth of about 25 km over the eastern part of the model, and to about 42 km depth under the Sierra Juárez, in good agreement with the crustal structure inferred by Nava and Brune (1982). At the bottom of the 2-D model is the mantle

extending down to 50 km-depth, modeled using a mass density of 3330 kg/m<sup>3</sup>.

The sedimentary fill in the Laguna Salada basin was modeled using several units that have increasing density with depth (Figure 9) and null magnetic susceptibility. The top unit has a mass density of 1800 kg/m<sup>3</sup>, and an average thickness of about 120 m, representing unconsolidated sediments. This is underlain by a 2000 kg/m<sup>3</sup> layer, about 800 m thick that extends all over the basin, down to a depth of about 1000 m and corresponds to the sequence of fine-grained lacustrine and fluvial deposits constituted by sand, gravel and shale (Figure 2). From about the central part of the basin to its eastern margin, the model features three layers, that show a regular increase of density with depth. The third layer, with

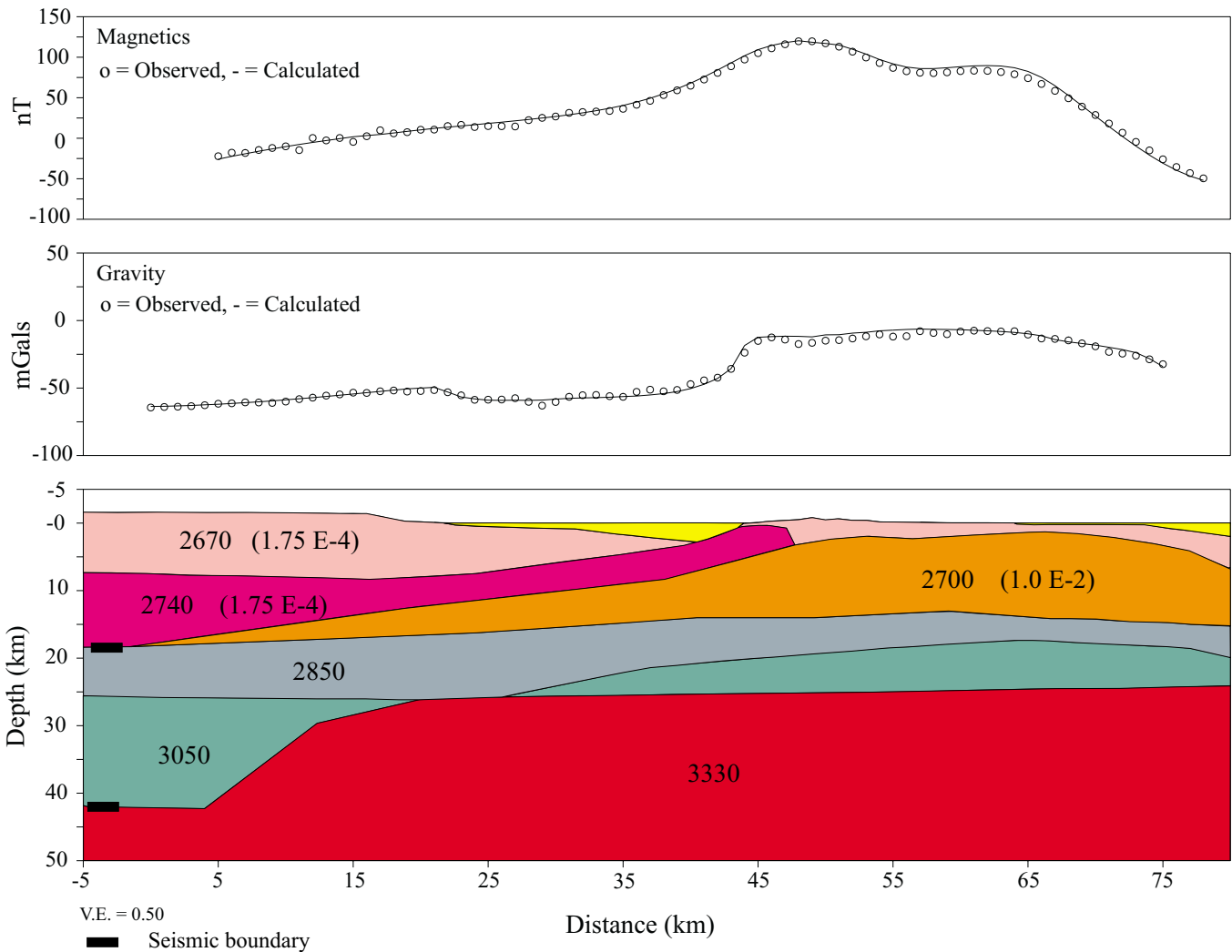


Fig. 8. 2-D geophysical model (A-A' in Figures 1, 4 and 5) between Sierra Juárez and Mexicali Valley. In the top panel is the residual magnetic anomaly; in the middle panel is the complete Bouguer gravity anomaly. Interpolated data denoted by open circles are spaced at one km. Continuous lines are the gravity/magnetic effect caused by the model shown in the bottom panel, where mass densities are labeled in units of kg/m<sup>3</sup>, and in parenthesis is magnetic susceptibility in SI units.

a mass density of 2300 kg/m<sup>3</sup>, represents several sequences of silts and sandstones, and granitic boulder-conglomerate and breccia (Figure 2). The fourth layer, with a mass density of 2400 kg/m<sup>3</sup>, represents fluvial arcotic sediments that may correspond to the Palm Spring Fm. (Figure 2). The layer at the bottom of the basin which has a mass density of 2500 kg/m<sup>3</sup> may corresponds to the Imperial Fm. Under the western portion of the Mexicali Valley, at the foothills of the Sierra Cucapá, the sedimentary infill starts with an up to 250-m thick layer, with a mass density of 2150 kg/m<sup>3</sup>. East of this unit is a 260 m thick layer, with a mass density of 2000 kg/m<sup>3</sup> representing unconsolidated sediments. This unit is underlay by a layer with a mass density of 2400 kg/m<sup>3</sup> that extends down to 1800 m depth in the model, and thickens to the east.

**CONCLUSIONS**

A 2-D model of the crustal structure, which accounts for gravity and magnetic data, was obtained between the Sierra Juárez and the western side of the Mexicali Valley. This model is robust in the sense that it explains both gravity and magnetic data, and it is constrained with depths to major seismic boundaries inferred from seismic refraction data, the Airy-Heiskanen model of isostatic compensation, spectral analysis of magnetic anomalies, mass density and magnetic susceptibility measurements carried out in samples from the Sierra Juárez, the Sierra Cucapá, and the Sierra El Mayor, and the density-log from well ELS-1. The inversion of the RA-PDS suggest that the mean depth to the bottom of a crustal magnetic layer lies at about 16 ± 2 km-depth in the region of

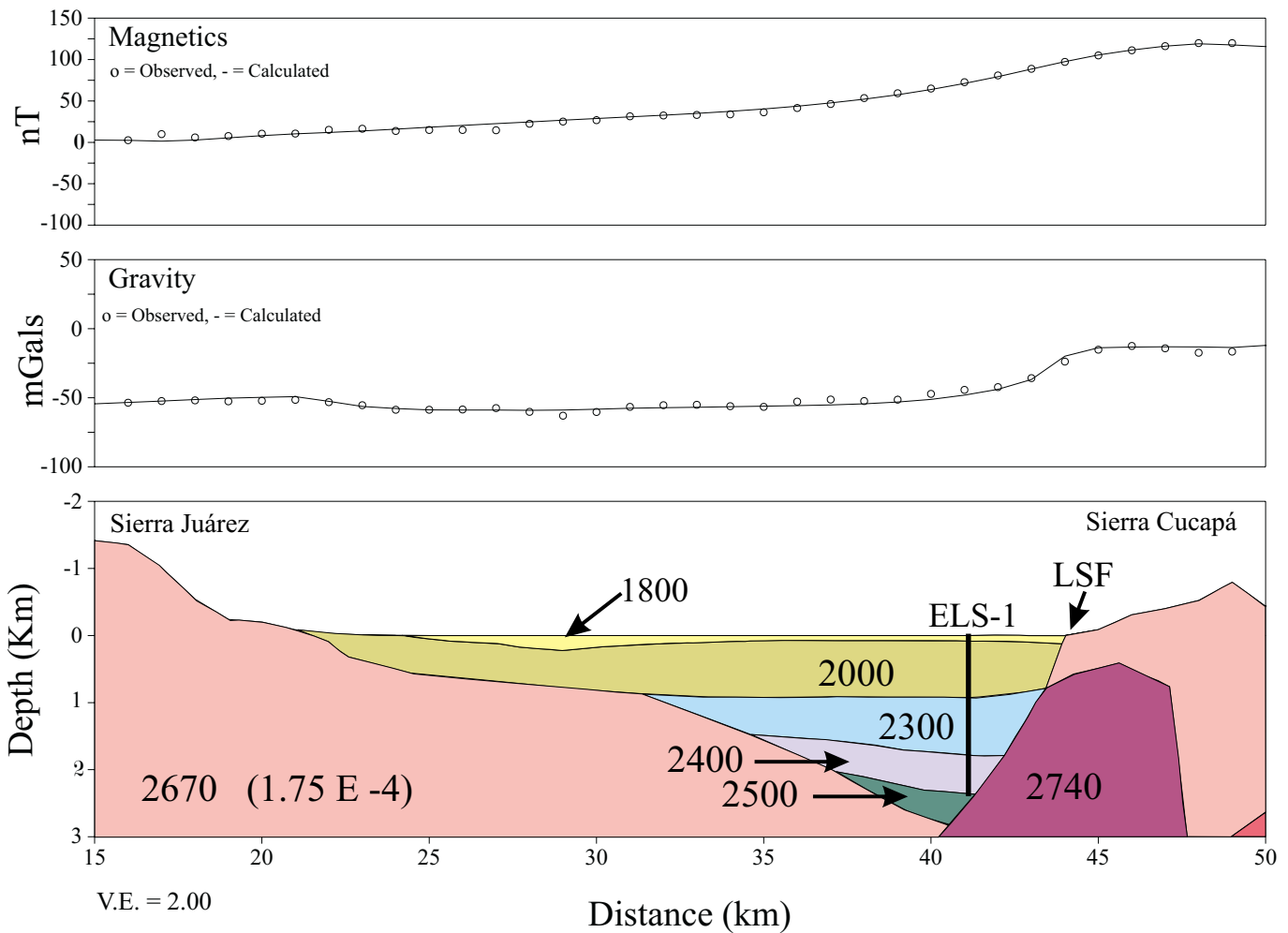


Fig. 9. Close up across the Laguna Salada basin, from the 2-D geophysical model shown in Figure 8. The location of the Laguna Salada fault (LSF) and depth reached by well ELS-1 is indicated. The explanation is as in Figure 8.

the Sierra Cucapá. Our 2-D model suggests a crust-mantle interface that lies at about 25 km depth under the Laguna Salada basin, the Sierra Cucapá, and the western side of the Mexicali valley, and a root under the Sierra Juárez at about 42 km depth. In this model, the thickness of the sedimentary blanket in the Laguna Salada Basin increases eastwardly, with a maximum depth of about 3 km, conforming a half-graben structure, in general agreement with holes drilled in the basin. This depth differs from former interpretations based on residual Bouguer gravity anomalies, by a factor of two.

The seismogenic zone in the study area comprises a crustal layer about 20 km thick, in good agreement with the depth to the base of the crustal magnetic layer inferred from spectral analysis of magnetic anomalies. This suggests that magnetite, with a Curie point temperature of ~580°C, carries the magnetization, that the Curie point isotherm depth nearly follows the brittle-ductile transition, and a normal gradient of temperature with depth of about 30°C/km, in agreement with the temperature measured at the bottom of holes drilled by CFE in the Laguna Salada basin.

The seismicity in the Laguna Salada basin occur as clusters of events that indicate zones of weakness, along which stresses are being released. Hypocenter depths of events occurring in the central part of the basin were mostly confined within a depth range of 2 to 6 km. Events deeper than 10 km were located at the basin margins, with a pattern that, within location errors, correlates well with the regional fault systems of the study area. Focal mechanisms deter-

mined in the Laguna Salada basin area provide evidence of transtensional deformation, in agreement with the regional tectonics.

### ACKNOWLEDGEMENTS

Fruitful conversations with Sergio Vázquez-Hernández and Javier Helenes-Escamilla provided insight about the sedimentary history in the Laguna Salada basin. We thank a review of a previous version of the present manuscript by Carlos Francisco Flores-Luna and Luis Alberto Delgado-Argote. We thank Edgardo Cañón-Tapia for helping us with the magnetic susceptibility measurements. Critical and constructive comments by one anonymous reviewer help us to improve the manuscript, and to nail out the relationship between the depth to the base of the seismogenic zone and the Curie point isotherm depth. Part of this study was carried out when JRH was at CICESE on sabbatical leave from the UABC. Víctor Manuel Frías-Camacho is acknowledge for drafting the figures.

### APPENDIX A. Magnetic susceptibility and mass density laboratory measurements.

A field survey was carried out in a region that includes the Sierra Juárez, the Sierra Cucapá, and the Sierra El Mayor, with the purpose of determine the range of variation and average values of both mass density and magnetic susceptibility, on granitic and metamorphic rocks outcropping in the study area. Although the sampling was non-uniform (Fig-

**Table A-1**

Wet-rock mass densities from the Laguna Salada region

Lithology	Number of samples	Range [kg/m <sup>3</sup> ]	Average [kg/m <sup>3</sup> ]
<u>Intrusive rocks</u>			
Granite	16	2440 - 2600	2580
Granodiorite	16	2490 - 2740	2640
Diorite	2	2590 - 2700	-
Tonalite	20	2490 - 2760	2650
<u>Metamorphic rocks</u>			
Schist	13	2390 - 3240	2700
Gneiss	2	2550 - 2560	-
Amphibolite	3	2740 - 3050	2910

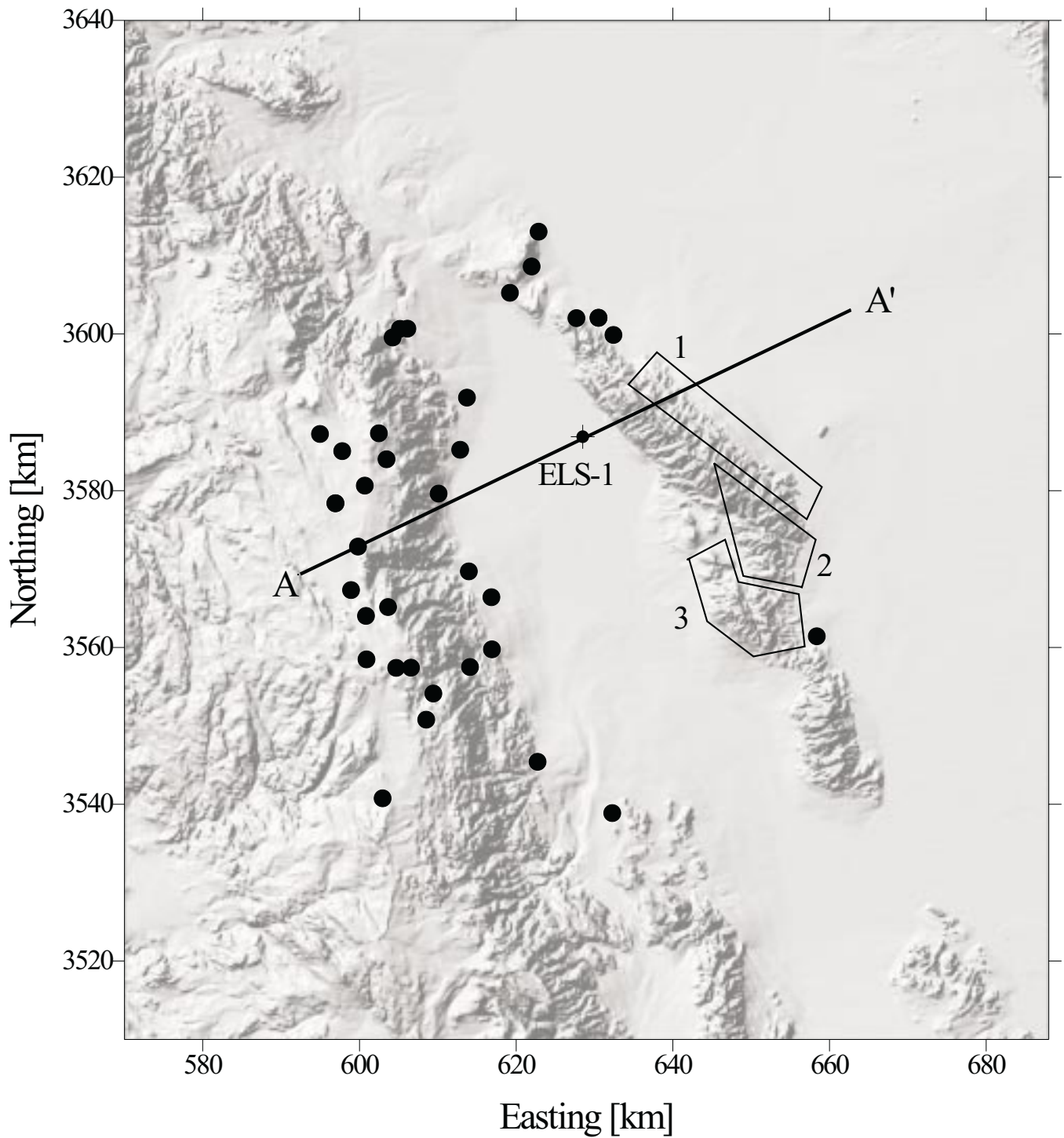


Fig. A-1. Location map of collected samples (solid circles) for mass density and magnetic susceptibility laboratory measurements. The polygon 1 shows the probable location of de Boerd (1981) samples in the Sierra Cucapá. The polygons 2 and 3 show the location of samples provided by colleagues currently working in the Sierra Cucapá and the Sierra El Mayor.

**Table A-2**

Magnetic susceptibilities of rocks from the Laguna Salada region

Lithology	Number of samples	Range [ $\times 10^{-4}$ SI]	Average [ $\times 10^{-4}$ SI]
<u>Intrusive rocks</u>			
Granite	16	1.1 - 27.5	7.8
Granodiorite	16	0.9 - 29.7	14.3
Diorite	2	2.8 - 26.4	-
Tonalite	20	2.5 - 40.9	18.0
<u>Metamorphic rocks</u>			
Schist	13	8.3 - 78.3	35.6
Gneiss	2	13.3 - 56.9	-
Amphibolite	3	35.5 - 73.7	68.1

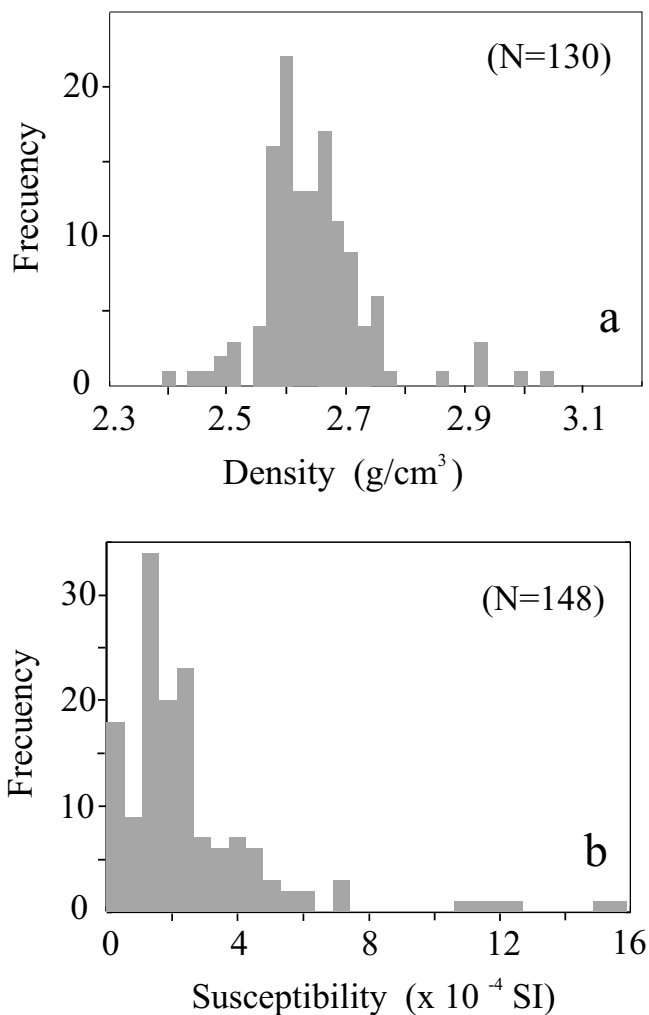


Fig. A-2. Histograms of mass density (a) and magnetic susceptibility (b) from samples collected in the Sierra Juárez, the Sierra Cucapá and the Sierra El Mayor.

ure A-1), the collected samples are representative of the wide variety of basement rocks outcropping in the study area.

We collected (18) metamorphic and (54) intrusive samples to measure its mass density and magnetic susceptibility in the laboratory using a precision balance and a Gico KLY-3 susceptibility meter. The mass density measurements (Table A-1) of intrusive rocks varies between 2440 and 2760  $\text{kg/m}^3$ , and for metamorphic rocks it varies between 2390 and 3240  $\text{kg/m}^3$ . The magnetic susceptibility was measured in situ using a Scintrex K-2 hand held susceptibility meter and most measurements were near the meter resolution ( $1 \times 10^{-4}$  SI units). The magnetic susceptibility laboratory measurements (Table A-2) of granitic rocks varies between  $0.9 \times 10^{-4}$  and  $40.9 \times 10^{-4}$  SI units, and for metamorphic rocks it varies between  $8.3 \times 10^{-4}$  and  $78.3 \times 10^{-4}$ .

Our collection was increased with rock samples provided by several colleges currently working in the region, and besides the location of samples is not a precise as desired, it helped us to construct the histograms of mass density and magnetic susceptibility shown in Figure A-2. The statistic analysis carried out on 130 samples indicates a normally distributed mass density that varies between 2400 – 2990  $\text{kg/m}^3$ , with a mean value of about  $2650 \pm 90 \text{ kg/m}^3$ . The mean mass density is slightly less than the standard density ( $2670 \text{ kg/m}^3$ ) used to compute the Bouguer anomaly. However, we observed that the mean density is skewed to low mass density values due to weathered coarse grained granitic samples. The statistical analysis of magnetic susceptibility, carried out on 148 samples, indicates a log normal (geometric) distribution that ranges between  $2.00 \times 10^{-5}$  to  $1.6 \times 10^{-3}$ , with a geometric mean magnetic susceptibility of about  $1.75 \pm 2.71 \times 10^{-4}$  SI units. This geometric mean is



close to the magnetic susceptibility values reported elsewhere for the eastern Peninsular Ranges Batholith.

Overall, the highest mass density and magnetic susceptibility values correspond to metamorphic rocks from La Rumorosa (north of Sierra Juárez) and the Sierra El Mayor. Density increases from felsic to mafic granitoids, the former located mainly in the Sierra Juárez and the later in the southern portion of the Sierra Cucapá.

## BIBLIOGRAPHY

- ÁLVAREZ-ROSALEZ, J. and M. GONZÁLEZ-LÓPEZ, 1995. Resultados de los pozos exploratorios en Laguna Salada, B.C., Sociedad Geológica Peninsular, Memorias de la III reunión internacional sobre la geología de la península de Baja California, La Paz, BCS, México, p. 4-5.
- ÁLVAREZ-ROSALEZ, J., 1991. Exploración geotérmica en Laguna Salada, B. C., Comisión Federal de Electricidad, Residencia General de Cerro Prieto, Residencia de Estudios, Departamento de Exploración. Mexicali, B.C., México, 14 pp.
- ANGELIER, J., B. COLLETTA, J. CHOROWICKS, L. ORTLIEB and C. RANGING, 1981. Fault tectonics of the Baja California Peninsula and the opening of the Sea of Cortés, Mexico. *J. Struct. Geol.*, 3, 347-357.
- ARELLANO-GUADARRAMA, J. F. and S. VENEGAS-SALGADO, 1992. Estado actual de la exploración geotérmica en Laguna Salada, B. C. *Geothermia. Rev. Mex. de Geoenergía*, 8, 331-356.
- AXEN, G. J., 1995. Extensional segmentation of the Main Gulf Scarpment, Mexico and United States. *Geology*, 23, 515-518.
- BARNARD, F. L., 1968. Structure and tectonics of the Sierra Cucapahs, Northeastern Baja California and Imperial county, California, Ph. D. thesis, 155 pp. University of Colorado, Boulder.
- BALSLEY, J. R. and A. F. BUDDINGTON, 1958. Iron-Titanium oxide minerals, rocks and aeromagnetic anomalies of the Adirondack area, New York, *Econ. Geology*, 53, 777-805.
- BLAKELY, R. J., 1995. Potential theory in gravity and magnetic applications, Cambridge University Press, 441 pp.
- CHÁVEZ, R. E., 1990. Gravity interpretation of the Laguna Salada basin, Baja California, México. *Geofís. Int.*, 29, 129,135.
- de BOER, J., 1979. Paleomagnetism of the Quaternary Cerro Prieto, Crater Elegante, and Salton Buttes volcanic domes in northern part of the Gulf of California rhombochasm. Proceedings of the Second Symposium on the Cerro Prieto geothermal field, Baja California, Mexico, 91-102.
- DELGADO-ARGOTE, L. A. and J. GARCÍA-ABDESLEM, 1999. Shallow Miocene basaltic magma reservoirs in the Bahía de Los Ángeles basin, Baja California, México. *J. Volcanol. Geotherm. Res.*, 93, 75-92.
- DORSEY, R. and A. MARTÍN-BARAJAS, 1999. Sedimentation and deformation in a Pliocene-Pleistocene transtensional supradetachment basin, Laguna Salada, north-west México. *Basin Research*, 11, 205-221.
- ESPINOSA-CARDEÑA, J. M., 1986. Panorama actual del potencial geotérmico del Valle de la Laguna Salada, B. C., México: Reporte Interno, 36 pp. Comisión Federal de Electricidad, Residencia General de Cerro Prieto, Residencia de Estudios, Departamento de Exploración. Mexicali, B.C., México.
- FONSECA, H. L. and A. RAZO-MONTIEL, 1979. Estudios gravimétricos, magnetométricos y de sísmica de reflexión en el campo geotérmico de Cerro Prieto: Memorias del Segundo Simposium sobre el Campo Geotérmico Cerro Prieto, LBL, Berkeley, California, p. 303-322.
- FREZ, J., F. NÚÑEZ, J. GONZÁLEZ, C. MONTANA and R. KELLER, 1994. A refraction profile between Blythe, Arizona, and Ensenada, B.C., *EOS, Trans. AGU*, 75, 485.
- GASTIL, R. G., R. P. PHILLIPS and E. C. ALLISON, 1975. Reconnaissance geology of the State of Baja California. *Geol. Soc. Am., Mem.* 140, 170 pp.
- GASTIL, R. G., D. KRUMMENACHER and J. MINCH, 1979. The record of Cenozoic volcanism around the Gulf of California. *Geol. Soc. Am., Bull.* 90, 839-857.
- GARCÍA-ABDESLEM, J. and J. M. ESPINOSA-CARDEÑA, 1994. Estudio gravimétrico regional sobre las sierras Juárez y Cucapá, Laguna Salada y Valle de Mexicali, Reporte Técnico, CICESE, División de

- Ciencias de la Tierra. Departamento de Geofísica Aplicada, 40 pp.
- GARCÍA-ABDESLEM, J. and G. E. NESS, 1994a. Inversion of the power spectrum from magnetic anomalies. *Geophysics*, 59, 391-401.
- GARCÍA-ABDESLEM, J. and G. E. NESS, 1994b. Crustal structure of the eastern part of the Maya Terrane from magnetic anomalies and magnetic power spectrum inversion. *Geofís. Int.*, 33, 399-420.
- GOLDSTEIN, N. E., M. J. WILT and D. J. CORRIGAN, 1984. Analysis of the Nuevo León magnetic anomaly and its possible relation to the Cerro Prieto magmatic-hydrothermal system. *Geothermics*, 13, 3-11.
- HENRY, C. D., 1989. Late Cenozoic Basin and Range structure in western México adjacent to the Gulf of California. *Geol. Soc. Am. Bull.*, 101, 1147-1156.
- HELENES-ESCAMILLA, J., 1999. Palinología y secuencias estratigráficas del pozo ELS-1, Laguna Salada, México. *Geotermia, Rev. Mex. de Geoenergía*, 15, 47-54.
- HUBERT, M. K., 1948. A line-integral method for computing the gravimetric effect of two-dimensional masses. *Geophysics*, 13, 215-22.
- INEGI (Instituto Nacional de Estadística, Geografía e Informática), 1980a, Carta Geológica Tijuana, I11-11, escala 1:250,000, Secretaría de Programación y Presupuesto, México D.F.
- INEGI (Instituto Nacional de Estadística, Geografía e Informática), 1980b, Carta Geológica Mexicali, I11-12, escala 1:250,000: Secretaría de Programación y Presupuesto, México D.F.
- KELM, L. D., 1971. A gravity and magnetic study of the Laguna Salada, B.C., M. Sc. Thesis, San Diego State University, 103 pp.
- LAY, T. and T. C. WALLACE, 1995. Modern global seismology, Academic Press.
- MUELLER, K. J. and T. K. ROCKWELL 1991. Late Quaternary structural evolution of the western margin of the Sierra Cucapah, northern Baja California. In: The Gulf and Peninsular Province of the Californias, Dauphin, J. P., and Simoneit, R. T. B., eds. Am. Assoc. Pet. Geol. Mem. 47, 249-260.
- NAVA, F. A. and J. A. BRUNE, 1982. An earthquake-explosion reversed refraction line in the Peninsular Ranges of southern California and Baja California Norte. *Seism. Soc. Am. Bull.*, 72, 1195-1206.
- O'CONNOR, J. E. and C. G. CHASE, 1989. Uplift of the Sierra San Pedro Mártir, Baja California, México. *Tectonics*, 8, 833-844.
- QUINTANILLA, A. L. and F. SUÁREZ-VIDAL, 1994. Fuente de calor en el campo geotérmico de Cerro Prieto y su relación con la anomalía magnética de Nuevo León, México. *Geofís. Int.*, 33, 575-584.
- RAMÍREZ-HERNÁNDEZ, J., M. VEGA-AGUILAR, C. CARREÓN-DIAZCONTI and J. A. REYES-LÓPEZ, 1994. Estudio gravimétrico de la zona geotérmica de Laguna Salada, B.C., Reporte Técnico, UABC, Instituto de Ingeniería, 50 pp.
- ROMERO-ESPEJEL, H., 1996. Geología estructural en el escarpe oriental de la Sierra Juárez, Baja California, México, Tesis de Maestría en Ciencias, CICESE, División de Ciencias de la Tierra.
- ROMERO-ESPEJEL, J. G. H. and L. A. DELGADO-ARGOTE, 1997. Granitoides en el noreste de Sierra Juárez, Baja California: una historia de emplazamiento para la parte norte del Batolito Oriental del Cretácico Tardío. *GEOS*, 17, 139-154.
- SAWLAN, M. G., 1991. Magmatic evolution of the Gulf of California Rift. In: Dauphin, J. P. and B. R. T. Simoneit (eds.), The Gulf and Peninsular Province of the Californias, Am. Assoc. Pet. Geol., Mem. 47, 301-369.
- SCHOLZ, C. H., 1968. The frequency-magnitude relation of microearthquakes in rock and its relation to earthquakes. *Bull. Seism. Soc. Am.*, 58, 399-415.
- SIEM, M. E., 1992. The structure and petrology of Sierra El Mayor, Northeastern Baja California, Mexico, M. Sc. Thesis, San Diego State University, 244 pp.
- SIEM, M. E. and R. G. GASTIL, 1994. Mid-Tertiary to Holocene extension associated with the development of the Sierra El Mayor metamorphic core complex, northeastern Baja California, Mexico. In: McGill, S. F. and Ross, T. M., eds. Geological investigations of an active margin, Geol. Soc. Am. Cordilleran Section guidebook, Redlands, California, San Bernardino County Museum Association, 107-119.

VÁZQUEZ-HERNÁNDEZ, S., 1996. Estratigrafía y ambientes de depósito de la secuencia sedimentaria al oriente de Laguna Salada, Baja California. Tesis de Maestría en Ciencias, CICESE, División Ciencias de la Tierra.

VELASCO-HERNÁNDEZ, J., 1963. Levantamiento gravimétrico en la Zona Geotérmica de Mexicali: Reporte Técnico, Consejo de Recursos Naturales no Renovables, México, D. F.

---

Juan García-Abdeslem, Juan Manuel Espinosa-Cardena, Luis Munguía-Orozco, Víctor Manuel Wong-Ortega and Jorge Ramírez-Hernández<sup>1</sup>

*CICESE (Centro de Investigación Científica y de Educación Superior de Ensenada), División de Ciencias de la Tierra, km 107, Carretera Tijuana-Ensenada, Ensenada, Baja California, 22860 México. jgarcia@cicese.mx.*

<sup>1</sup>*UABC (Universidad Autónoma de Baja California), Instituto de Ingeniería, Mexicali, B. C., México.*